Journal of Catalysis **199,** 309–317 (2001)
doi:10.1006/jcat.2001.3190, available online at http://www.idealibrary.com on IDEAL®

Partial Oxidation of Methane to Synthesis Gas over Alkaline Earth Metal Oxide Supported Cobalt Catalysts

H. Y. Wang and E. Ruckenstein[1]

Department of Chemical Engineering, State University of New York at Buffalo, Amherst, New York 14260

Received September 15, 2000; accepted January 29, 2001; published online March 27, 2001

The partial oxidation of methane to synthesis gas was investigated over the alkaline earth metal oxide supported Co catalysts. Only MgO has proved to be a suitable support. The reaction behavior of the MgO-supported Co catalysts was significantly influenced by the calcination temperature (T_c) and Co loading. The 24 wt% Co/MgO catalyst precalcined at 800°C provided a high and stable activity; those precalcined at higher temperatures provided a lower stable activity and those precalcined at lower temperatures a lower stability. Because of the two oxidative states of Co, the structural characteristics of the Co catalysts are strongly affected by the nature of the support, calcination temperature, and Co loading. In the 24 wt% MgO-supported catalysts, only a solid solution of CoO and MgO was identified for $T_c \geq 800$°C, while one or two of the following compounds, Co_3O_4 and $MgCo_2O_4$, were additionally detected for $T_c < 800$°C. Correlations among the species present in the catalyst, its reducibility, and its catalytic performance were established.

Key Words: **partial oxidation of methane; synthesis gas; Co catalyst; effect of support; effect of calcination temperature; effect of Co loading.**

1. INTRODUCTION

The partial oxidation of methane, which was first investigated by Prettre *et al.* as early as 1946 (1), has gained renewed interest during the past years (2–22). The catalysts that have been reported to be active and selective toward the synthesis gas formation were mainly supported noble metals, such as Rh, Ru, Pd, Pt (2–8), supported Ni (9–17), and Co (16–18) catalysts, as well as some pyrochlore type oxides, such as $Ln_2Ru_2O_7$ (19, 20), and perovskite type oxides, such as $LaMO_3$ (M = Ni, Rh, Co, Cr) (21, 22).

Compared to the noble-metal based catalysts, the Ni- and Co-based catalysts are particularly promising due to their low prices. In recent papers, Ni/MgO catalysts, obtained through the reduction of NiO–MgO solid solutions, were reported to provide high and stable activities for the methane conversion to synthesis gas via CO_2 reforming (23), partial oxidation (12, 15), and their combination (24). Like NiO, CoO can also form an "ideal" solid solution over the entire mole fraction range with MgO (25, 26). However, unlike Ni, Co has two oxidative states (Co^{2+} and Co^{3+}). Consequently, additional species can be generated between the cobalt and magnesium oxides during the preparation of the catalyst, which are expected to depend on the preparation conditions, such as calcination temperature and metal loading. The species present in a catalyst affect its reducibility and the size and morphology of the metal particles thus generated and hence the catalytic pattern of the catalyst. Of course, during reaction other species may form as well in the catalyst. It is therefore of interest to identify the species formed in the catalyst and their role in the catalytic process. For this purpose, the reaction behavior of the Co/MgO catalysts in the partial oxidation of methane was investigated as a function of calcination temperature and Co loading. For comparison purposes, the Co catalysts supported on the other alkaline earth metal oxides were also included in the investigation.

2. EXPERIMENTAL

2.1. Catalyst Preparation

The catalysts were prepared by impregnating the supports (MgO, CaO, SrO, and BaO) with aqueous solutions of $Co(NO_3)_2 \cdot 6H_2O$, followed by overnight drying at 110°C. The samples were then calcined in the open air of a furnace for 8 h at 800°C, when CaO, SrO, and BaO were used as supports, and at various temperatures between 500 and 1000°C, when MgO was employed. The calcined catalysts are denoted as Co(O)/MO (M = Mg, Ca, Sr, or Ba) and the catalysts reduced in H_2 as Co/MO. Co loading means wt% Co in the completely reduced catalyst.

2.2. Catalytic Reaction

All the catalysts were tested under atmospheric pressure and at a $T_{furnace}$ of 850°C in a fixed-bed vertical quartz reactor (i.d. 3 mm), which was operated in a downflow mode with the catalyst held on a quartz wool bed. The reduction

[1] To whom correspondence should be addressed. Fax: +1-716-645-3822. E-mail: feaeliru@acsu.buffalo.edu.

0021-9517/01 $35.00

of the catalyst was carried out by increasing the temperature from room temperature to 600°C at a rate of 20°C/min and from 600 to 850°C at a rate of 10°C/min, in a H_2 flow (20 ml/min), without holding at 850°C. After reduction, the feed gases ($CH_4/O_2 = 2/1$) were introduced into the catalyst bed at a flow rate of 60 ml/min. The reactants and products were analyzed with an on-line gas chromatograph equipped with a Porapak Q column. An ice-cold trap was located between the reactor exit and the GC sampling valve to remove the water formed during reaction.

2.3. Catalyst Characterization

2.3.1. BET surface area and the exposed Co surface area. The BET surface areas of the calcined catalysts, determined via nitrogen adsorption using a Micromeritics ASAP2000 instrument, are listed in Table 1.

The exposed Co metal surface area of the reduced catalyst was determined by CO pulse adsorption in a quartz tube (i.d. 4 mm) at room temperature, assuming a 1/1 stoichiometry. Fifty milligrams of the calcined catalyst powder was charged and its reduction was carried out as described in the previous section. After reduction, the catalyst was purged with an ultra high purity carrier gas (He, 35 ml/min) at 850°C for 0.25 h, and then the sample was cooled to room temperature. CO pulses (10 μl per pulse) were then injected in the carrier gas and passed over the reduced catalyst. The CO uptake in each pulse was monitored using a thermal conductivity detector (TCD).

2.3.2. CH_4 decomposition. The decomposition of pure methane over the reduced catalyst was carried out in a quartz tube (i.d. 4 mm) reactor containing 25.0 mg of calcined catalyst. After reduction, which was carried out as described previously, the catalyst was purged with a carrier gas (He, 35 ml/min) at 850°C for 0.25 h and then pulses of CH_4 (250 μl) were injected in the carrier gas. The products were analyzed with an on-line gas chromatograph equipped with a TCD and a Porapak Q column.

2.3.3. Temperature-programmed reduction (TPR). During each TPR run, a high-purity 2.5% H_2/Ar mixture (35 ml/min) was passed over a calcined sample in a vertical quartz tube reactor (i.d. 4 mm). The sample (10.0 or 20.0 mg) was held on a quartz wool bed and the temperature of the sample was increased from 40 to 1000°C at a rate of 20°C/min. The water, formed during reduction, was trapped in a Hydro-Purge II column. The hydrogen consumed in TPR was monitored continuously with a TCD, which was calibrated using known amounts of CoO and Co_3O_4.

2.3.4. X-ray powder diffraction (XRD). XRD, performed with a Siemens D500 X-ray diffractometer using filtered Cu$K\alpha$ radiation, was used to identify the major phases of the calcined catalysts.

TABLE 1

Physical Data for the Supported Co Catalysts

Support	Co loading (wt%)	Calcination temp. (°C)	Surface area[a] (m^2/g cat.)	Co surface area[b] (m^2/g cat.) × 100
MgO	6	800	26	7
MgO	12	800	22	7
MgO	24	500	58	201
MgO	24	700	28	52
MgO	24	800	20	9
MgO	24	900	11	5
MgO	24	1000	5	—[c]
MgO	36	800	14	8
MgO	48	800	12	25
CaO	24	800	5	79
SrO	24	800	4	8
BaO	24	800	1	—[c]

[a] For the calcined catalysts.
[b] For the reduced catalysts.
[c] Too small to be detected.

3. RESULTS

3.1. Partial Oxidation of Methane to Synthesis Gas

3.1.1. Comparison of the catalysts supported on different alkaline earth metal oxides. The time-dependent conversions of CH_4 and O_2 and selectivities to CO and H_2 of the 24 wt% Co catalysts supported on MgO, CaO, SrO, and BaO precalcined at 800°C are plotted in Fig. 1. Over the Co/MgO, after an activation period of about 2 h, the conversion of CH_4 and selectivities to CO and H_2 remained high and unchanged during the period of study of 120 h and a H_2/CO ratio of about 2 was obtained. Over CaO-, SrO-, and BaO-supported catalysts the initial (after 8 min) conversions of CH_4 and selectivities to CO and H_2 were much lower than those over MgO and, in addition, notable deactivation was observed.

3.1.2. Effect of calcination temperature on the MgO-supported Co catalysts. The time-dependent activities of the MgO-supported catalysts precalcined at temperatures between 500 and 1000°C are plotted in Fig. 2. Only the conversion of CH_4 is presented because that of O_2 was always 100%, and only the selectivity to CO is plotted because that to H_2 followed the same pattern. The results can be summarized as follows: (i) the catalysts precalcined at temperatures $\geq$800°C exhibited stable activities and selectivities, which decreased with increasing calcination temperature; (ii) some deactivation with time on stream occurred over the catalysts precalcined at 500 and 700°C; (iii) the initial conversion of methane and CO selectivity decreased with increasing calcination temperature from 500 to 1000°C; (iv) activation periods were observed, particularly for the catalysts calcined at temperatures $\geq$800°C.

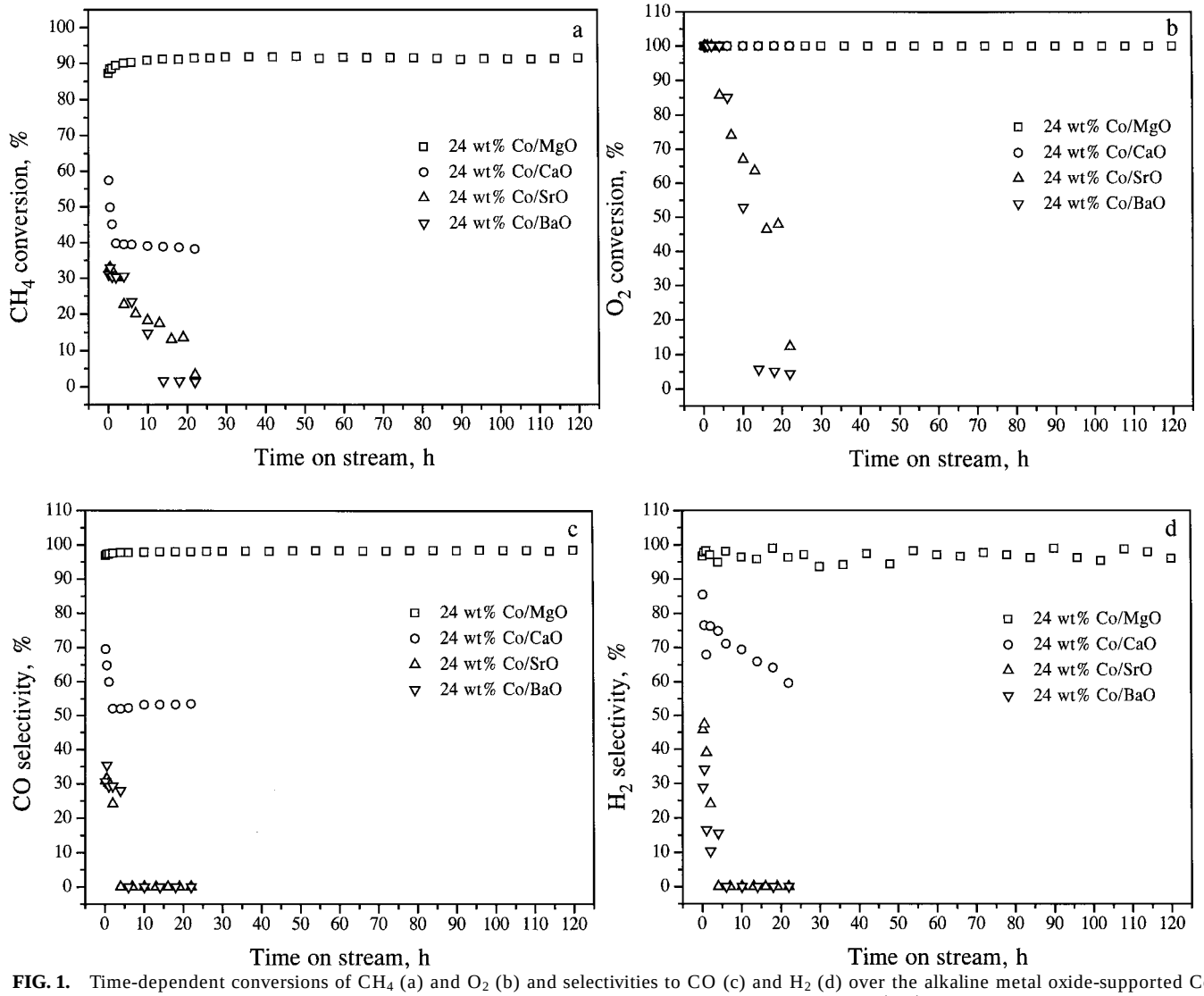

FIG. 1. Time-dependent conversions of CH_4 (a) and O_2 (b) and selectivities to CO (c) and H_2 (d) over the alkaline metal oxide-supported Co catalysts (precalcined at 800°C). $P = 1$ atm, $T_{\text{furnace}} = 850$°C, $CH_4/O_2 = 2.0$, space velocity = 720,000 ml h^{-1} g^{-1}.

3.1.3. Effect of Co loading on the MgO-supported Co catalysts. The time-dependent activities of the MgO-supported catalysts with loadings between 6 and 48 wt% (precalcined at 800°C) are plotted in Fig. 3, which shows: (i) over the 6 wt% catalyst, the conversion of CH_4 was below 20%, and no CO and H_2 were formed; (ii) over those with loadings ≥12 wt%, the conversion of CH_4 was above 80%, and CO and H_2 were formed with high selectivities (>90%); (iii) with the increase in Co loading from 12 to 24 wt%, the conversion of CH_4 and the selectivity to CO increased somewhat, but remained almost unchanged with the further increase from 24 to 48 wt%.

3.1.4. Effect of the amount of catalyst. As shown in Fig. 4, over the 24 wt% Co/MgO catalyst (precalcined at 800°C), the conversion of CH_4 and the selectivity to CO increased with increasing amount of catalyst from 1.5 to 5.0 mg, but remained almost unchanged when the amount was increased from 5.0 to 15.0 mg.

3.2. Physicochemical Characterization

3.2.1. The exposed metallic Co surface area of the reduced catalyst. As shown in Table 1, for the 800°C calcined Co catalysts supported on different alkaline earth metal oxides, the exposed metal surface area after reduction decreased in the sequence CaO ≫ MgO ≈ SrO ≫ BaO. For the last support, the Co surface area was too small to be detected. For the Co/MgO catalysts, Table 1 shows that for the same loading (24 wt%), the exposed Co surface area decreased with increasing calcination temperature from 500 to 1000°C; for the same calcination temperature (800°C), it was almost the same for loadings between 6 and 36 wt%, but increased notably with increasing Co loading from 36 to 48 wt%.

3.2.2. Surface carbon (C) formed in the CH_4 decomposition. The decomposition of CH_4 pulses over the reduced catalysts was carried out at 850°C and the amount of surface carbon (C) generated was calculated from the carbon

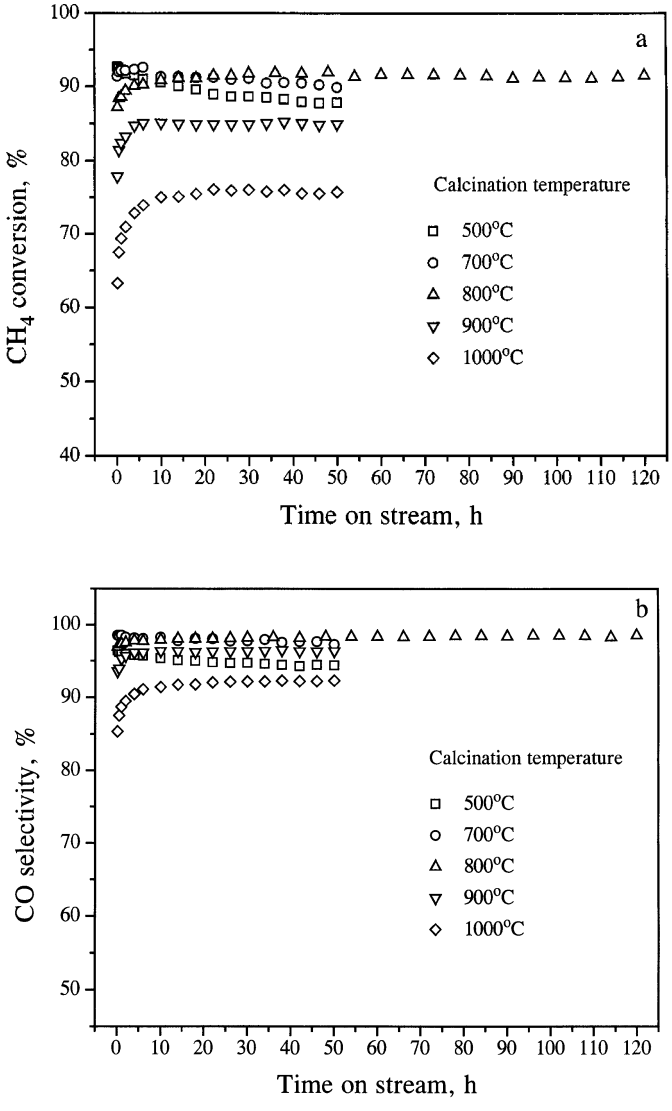

FIG. 2. Time-dependent conversion of CH_4 (a) and selectivity to CO (b) over the 24 wt% Co/MgO catalysts precalcined at various temperatures. $P = 1$ atm, $T_{furnace} = 850°C$, $CH_4/O_2 = 2.0$, space velocity = 720,000 ml h^{-1} g^{-1}.

balance. Table 2 shows that, for the 800°C calcined Co catalysts supported on different alkaline earth metal oxides, the amount of C accumulated during the same period over MgO was comparable to that over BaO, but much lower than those over CaO and SrO. The low carbon deposition over BaO was due to the low exposed metal surface area. Table 2 also shows that, for the 24 wt% Co/MgO catalysts, the amount of C formed decreased monotonically with increasing calcination temperature from 500 to 1000°C.

3.2.3. Reduction characteristics of the calcined supported Co catalysts. The TPR spectra of the 800°C calcined 24 wt% Co catalysts supported on different alkaline earth metal oxides are plotted in Fig. 5. For Co(O)/MgO, a peak started to form at a temperature higher than 800°C (Fig. 5a). A single peak at about 540°C was observed for Co(O)/CaO (Fig. 5b), and two peaks, one (the main) at about 505°C and the other one as a shoulder at about 710°C for Co(O)/SrO (Fig. 5c). Two peaks, one (the main) at about 455°C and the other one as a shoulder at about 790°C, were noted for Co(O)/BaO (Fig. 5d). The reduction extent over the MgO supported catalyst after TPR was estimated to be below 5%, while nearly 100% reduction was reached over the other alkaline earth metal oxide supported ones.

The TPR profiles of the 24 wt% Co(O)/MgO catalysts calcined at temperatures between 500 to 1000°C are presented in Fig. 6. The 500°C calcined 24 wt% Co(O)/MgO exhibited two reduction peaks, one at about 320°C and the other at about 695°C. The reduction extent of the sample

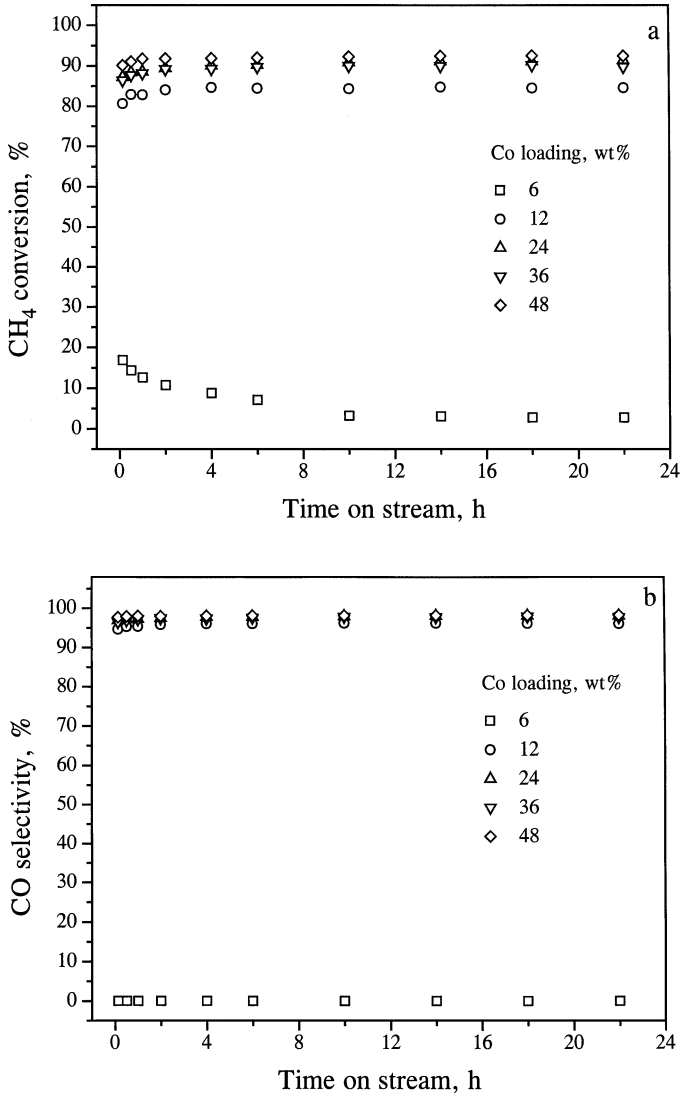

FIG. 3. Time-dependent conversion of CH_4 (a) and selectivity to CO (b) over the Co/MgO catalysts (precalcined at 800°C) with different Co loadings. $P = 1$ atm, $T_{furnace} = 850°C$, $CH_4/O_2 = 2.0$, space velocity = 720,000 ml h^{-1} g^{-1}.

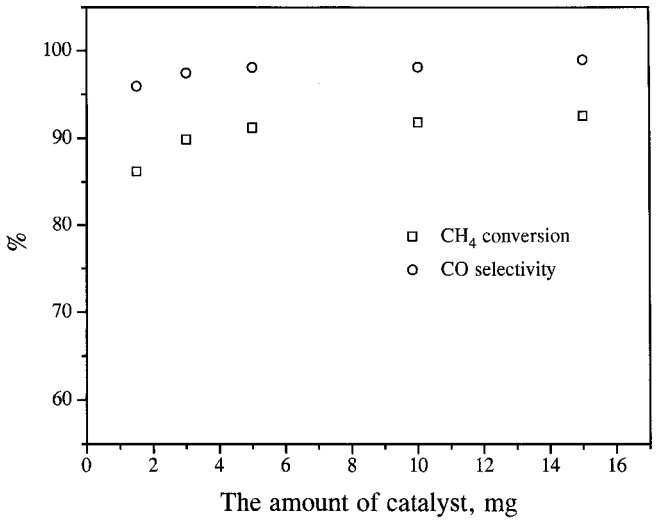

FIG. 4. Effect of the amount of catalyst on the CH_4 conversion and CO selectivity of the 24 wt% Co/MgO (precalcined at 800°C). Data obtained after 22 h of reaction; reaction conditions: $P = 1$ atm, $T_{furnace} = 850$°C, $CH_4/O_2 = 2.0$ (60 ml/min).

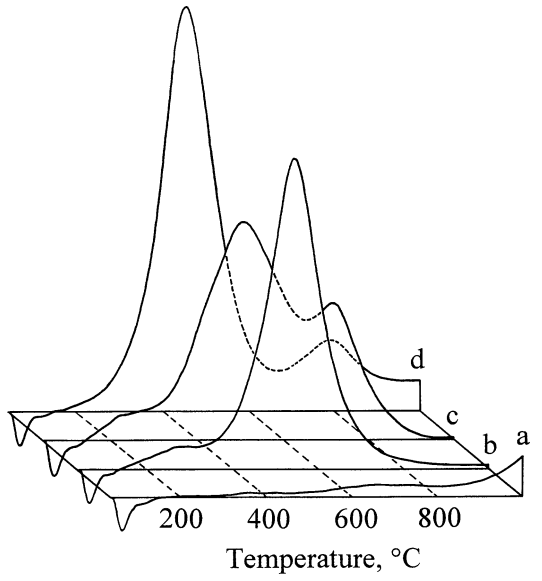

FIG. 5. TPR profiles of the 800°C calcined 24 wt% Co catalysts supported on MgO (a), CaO (b), SrO (c), and BaO (d).

was below 30%. At the calcination temperature of 700°C, in addition to a wide single peak at 430°C, a peak started to form at a temperature higher than 800°C. For calcination temperatures ≥800°C only a single peak started to form at temperatures higher than 800°C.

For all the 800°C calcined Co(O)/MgO catalysts with Co loadings between 6 and 24 wt%, a peak started to form at a temperature higher than 800°C; an additional low-temperature reduction peak between 380 and 430°C was observed over the catalysts with Co loadings of 36 and 48 wt%.

3.2.4. Compounds present in the calcined supported Co catalysts. The Co-containing species present in the calcined catalysts were identified by combining the XRD and TPR results. The data and the assignments of the XRD patterns for the calcined Co catalysts are listed in Table 3. For the 800°C calcined 24 wt% Co(O)/MgO, the XRD patterns could be attributed to (Co, Mg)O (solid solution of CoO and MgO) and/or MgO (Table 3). The reduction peak that started to form at a temperature higher than 800°C (Fig. 5a) allowed us to conclude that a solid solution was formed. $Ca_3Co_4O_9$ was identified over Co(O)/CaO, in agreement with the TPR spectrum (Fig. 5b) which provided a single reduction peak. Only $SrCoO_{2.52}$ was detected over Co(O)/SrO, while two reduction peaks were present in the TPR spectrum (Fig. 5c). Most likely, the amount of the species corresponding to the TPR shoulder was too small to be detectable by XRD. Thus, the major phase present in the Co(O)/SrO was $SrCoO_{2.52}$. Similarly, the major phase present in the Co(O)/BaO was found to be $BaCoO_{2.8}$.

The XRD results for the 500°C calcined 24 wt% Co(O)/MgO catalyst can be assigned to Co_3O_4 and/or $MgCo_2O_4$, as well as to (Co, Mg)O and/or MgO (Table 3).

TABLE 2

Amount of Carbon Deposited during CH_4 Decomposition over the Reduced Supported Co (24 wt% Loading) Catalysts at 850°C

Support	Calcination temp. (°C)	C formed during different periods (μmol) First pulse	First 3 pulses	First 5 pulses	First 10 pulses	First 20 pulses
MgO	500	8.2	16.8	19.1	23.5	29.4
MgO	700	6.5	9.4	11.0	14.1	18.4
MgO	800	2.2	5.1	6.6	9.7	14.9
MgO	900	1.5	3.3	4.0	5.8	9.0
MgO	1000	1.2	2.8	3.6	4.9	6.9
CaO	800	9.0	22.7	28.2	36.1	45.7
SrO	800	6.6	10.1	12.7	17.1	22.8
BaO	800	2.2	4.3	6.0	9.6	16.3

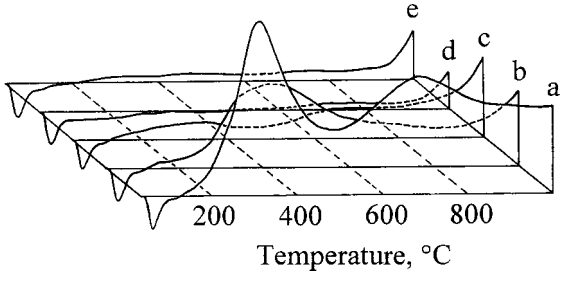

FIG. 6. TPR profiles of the 24 wt% Co(O)/MgO catalysts calcined at (a) 500, (b) 700, (c) 800, (d) 900, and (e) 1000°C.

TABLE 3

Data and Assignments of XRD Patterns of the Calcined Supported Co Catalysts

Support	Co loading (wt%)	Calcination temp. (°C)	*d* (Å)	Assignments	Co-containing species present[a]
MgO	24	500	2.438, 1.440, 2.869, 1.560, 2.038; 2.106, 1.490, 1.216,1.270, 2.438	Co_3O_4 and/or $MgCo_2O_4$; (Co, Mg)O and or MgO	Co_3O_4 and $MgCo_2O_4$; (Co, Mg)O
MgO	24	700	2.436, 1.430, 2.859, 1.557, 2.020; 2.108, 1.491, 1.218, 1.271, 2.436	Co_3O_4 and/or $MgCo_2O_4$; (Co, Mg)O and/or MgO	Co_3O_4; (Co, Mg)O
MgO	24	800	2.110, 1.493, 1.272, 1.218, 2.438	(Co, Mg)O and/or MgO	(Co, Mg)O
MgO	48	800	2.111, 1.493, 1.274, 1.219, 2.438; 2.438, 1.429, 2.860, 1.556, 2.022, 1.652	(Co, Mg)O and/or MgO; Co_3O_4 and/or $MgCo_2O_4$	(Co, Mg)O; Co_3O_4
CaO	24	800	2.686, 2.273, 3.587, 2.406, 2.083, 1.878	$Ca_3Co_4O_9$	$Ca_3Co_4O_9$
SrO	24	800	2.740, 3.105, 2.051, 1.642, 1.582, 1.372	$SrCoO_{2.52}$	$SrCoO_{2.52}$
BaO	24	800	3.401, 2.806, 2.164, 1.711, 2.379, 1.454	$BaCoO_{2.8}$	$BaCoO_{2.8}$

[a] Concluded by combining TPR and XRD results.

Since Co_3O_4 can be reduced in H_2 below 500°C (27, 28) and a complete reduction of (Co, Mg)O requires a temperature higher than 1000°C (Fig. 5a), the peak at about 320°C can be attributed to Co_3O_4 and the one at about 695°C to $MgCo_2O_4$. Though only two reduction peaks were observed for this catalyst (Fig. 6a), its reduction extent below 30% suggested that (Co, Mg)O was also present. Its reduction peak was not observed most likely because the upper-limit temperature during the TPR experiment was not high enough. Similarly, the XRD patterns (Table 3) coupled with the TPR spectra (Figs. 6b and 6c) indicated that Co_3O_4 and (Co, Mg)O were present in the 700°C calcined catalyst and solely (Co, Mg)O in the 800°C calcined catalyst. Based on the similarity of the TPR spectra among the catalysts calcined at temperatures ≥800°C, one can conclude that only (Co, Mg)O was present in the 900 and 1000°C calcined catalysts.

The XRD patterns (Table 3) coupled with the TPR spectrum (Fig. 7e) indicated that Co_3O_4 and (Co, Mg)O were present in the 48 wt% Co(O)/MgO(800°C) catalyst. Among the 800°C calcined catalysts with different Co loadings, the TPR spectra for loadings of 4 and 12 wt% were similar to that for 24 wt%, and the TPR spectrum for the 36 wt% was similar to that for the 48 wt% (Fig. 7). Consequently, one can conclude that Co_3O_4 and (Co, Mg)O were present in the 36 and 48 wt% Co(O)/MgO(800°C) catalysts, but only (Co, Mg)O in the Co(O)/MgO(800°C) catalysts with Co loadings ≤24 wt%.

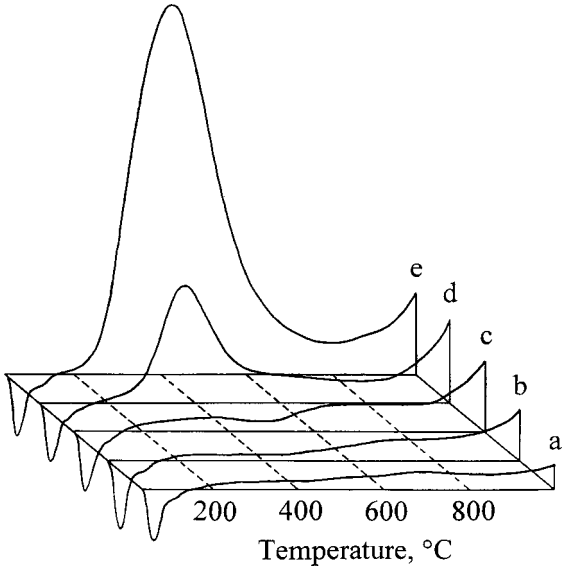

FIG. 7. TPR profiles of the 800°C calcined Co(O)/MgO catalysts with Co loadings of 6 wt% (a), 12 wt% (b), 24 wt% (c), 36 wt% (d), and 48 wt% (e).

4. DISCUSSION

4.1. Influence of Support, Calcination Temperature, and Co Loading on the Species Present in the Co Catalysts

First, it should be noted that for the same calcination conditions and the same Co loading the species formed in Co catalysts are dependent on the nature of the support. MgO, CaO, SrO, BaO, and CoO all have a NaCl-type structure. However, only MgO has a lattice parameter and bond distance close to CoO (Table 4). As a result, a solid solution of CoO and MgO was formed in the MgO-supported catalyst

TABLE 4

Crystal Data for NaCl Type Metal Oxides (29)

Compound	*a* (Å)	*A–B* distance (Å)
MgO	4.2112	2.11
CaO	4.8105	2.40
SrO	5.1396	2.57
BaO	5.5391	2.77
CoO	4.2603	2.13

after calcination at 800°C, while a compound, in which Co was present as Co^{n+} ($n \geq 3$), was present as major phase in the other alkaline earth metal oxide supports (Table 3).

Second, one should emphasize that the species present in the MgO supported catalysts are strongly affected by the calcination temperature and Co loading. Because of the two oxidative states of Co, other species can be generated between cobalt and magnesium oxides besides the solid solution. Indeed, depending upon the calcination temperature and Co loading, XRD (Table 3) and TPR (Figs. 6 and 7) brought evidence for the existence of one, two, or three of the following compounds: Co_3O_4, $MgCo_2O_4$, and (Co, Mg)O. For the 24 wt% Co catalysts, Co_3O_4, Co_2MgO_4, and (Co, Mg)O were present in the 500°C calcined catalyst, Co_3O_4 and (Co, Mg)O in the 700°C calcined one, and solely (Co, Mg)O in the catalysts calcined at temperatures ≥800°C. For the 800°C calcined Co(O)/MgO catalysts, Co_3O_4 and (Co, Mg)O were present in the 36 and 48 wt% catalysts, but only (Co, Mg)O in the catalysts with Co loadings ≤24 wt%.

4.2. *Influence of the Species Present on the Reducibility of Co Catalysts*

The reducibility of a catalyst is directly related to the compounds formed during calcination. Due to the irreducibility of MgO and because the oxygen belonging to Co interacts also with Mg, it is difficult to reduce the CoO dispersed in the lattice of MgO. Indeed, the 800°C calcined 24 wt% Co(O)/MgO required the highest reduction temperature (Fig. 5) and its extent of reduction after the TPR was below 5%. For this reason, the exposed Co surface area over the Co/MgO was much lower than that over the Co/CaO (Table 1). Most likely, the low exposed Co surface area over the Co/SrO and Co/BaO (Table 1) was caused by the sintering of the metallic crystallites and their burying induced by the sintering of SrO and BaO.

The reducibility of the three Co-containing species identified in the MgO-supported catalysts decreased in the sequence Co_3O_4 > Co_2MgO_4 > (Co, Mg)O. Consequently, under the conditions that favor the formation of a solid solution the percentage of cobalt that can be reduced to metal is expected to decrease. Indeed, the exposed metal surface area of the 24 wt% Co/MgO catalysts decreased monotonically as the calcination temperature was increased from 500 to 1000°C (Table 1).

4.3. *The Partial Oxidation of Methane to Synthesis Gas*

4.3.1. Effect of support on the reaction behavior of Co catalysts. Among the four alkaline earth metal oxides investigated, only MgO provided a high and stable activity during the period of study of 120 h; various extents of deactivation were observed over CaO, SrO, and BaO (Fig. 1). The carbon deposition and the metal sintering are the main causes for catalyst deactivation in the partial oxidation of methane. Sintering decreases not only the number of active sites, but also accelerates the carbon deposition, since large metal ensembles stimulate coke formation (30).

The size and morphology of metal clusters in the reduced catalysts is strongly affected by its reducibility. The higher the reducibility, the larger the size of metal particles is expected to be. When only a solid solution is present, hence for an MgO supported catalyst precalcined at $T_c \geq 800$°C, the size of the metal clusters is expected to be small. Parmaliana *et al.* brought transmission electron microscopy (TEM) evidence for a quasi-uniform distribution of small Ni particles ($d = 25$ Å) originated through the reduction of Ni^{2+} ions dispersed in the MgO matrix of a NiO–MgO solid solution (31). Being small, the clusters do not favor coke formation. Indeed, Table 2 indicates that the carbon deposition during the decomposition of pure CH_4 was much lower over the Co/MgO than over the Co/CaO and Co/SrO (while the carbon deposition was almost equally low over the Co/BaO, no metallic sites were present in this catalyst). Being extracted from the substrate, the generated metallic clusters remain partially embedded into the MgO lattice. Parmaliana *et al.* brought TEM evidence that such embedding is present in the reduced NiO–MgO solid solution systems (31). Being partially embedded into the MgO lattice, they are more resistant to sintering than the crystallites supported on the conventional supports (32). In conclusion, the high stability of the Co/MgO catalyst is related to the formation of a solid solution of CoO and MgO during calcination.

4.3.2. Effect of calcination temperature on the reaction behavior of Co/MgO catalysts. The calcination temperature has a significant influence on the stability of the Co/MgO catalysts. The 24 wt% Co catalysts precalcined at temperatures ≥800°C exhibited stable activities during the period of study, while some deactivation was observed over the catalysts precalcined at 500 and 700°C (Fig. 2). The XRD and TPR indicated that only the solid solution was present in the catalysts calcined at ≥800°C and that Co_3O_4 and $MgCo_2O_4$ were additionally present in the 500°C and Co_3O_4 in the 700°C calcined ones (Table 3). Being more reducible than the solid solution, they generated large metal clusters that stimulated carbon deposition. Indeed, as shown in Table 2, the carbon deposition during the CH_4 decomposition was much greater over the 500 and 700°C calcined catalysts than over those calcined at temperatures ≥800°C. In addition, due to the relatively weak interactions between these clusters and support, enhanced sintering occurred. Carbon deposition and sintering were responsible for deactivation.

On the other hand, with increasing calcination temperature from 500 to 1000°C, the initial conversion of methane in partial oxidation of methane decreased (Fig. 2). This reflects the trend of the exposed Co surface area (Table 1) and implies that the metallic sites are the active sites for the synthesis gas formation. The concentration of CoO near the surface decreased with increasing calcination temperature,

because the higher the calcination temperature the deeper is the penetration of CoO into the MgO lattice. For this reason, fewer metallic sites were present on the surface of the catalysts precalcined at higher temperatures and the initial activity decreased with increasing calcination temperature. In addition, an activation period can be noted over the catalysts precalcined at temperatures $\geq$800°C (Fig. 2a), indicating that additional metallic sites were generated during reaction via the reduction of the solid solution by CH_4 and/or H_2. Consequently, the solid solution catalyst acts like a "reservoir" which can provide additional active metallic sites during reaction.

4.3.3. Effect of Co loading on the reaction behavior of Co/MgO catalysts. The reaction behavior of Co/MgO catalysts is affected by Co loading. As shown in Fig. 3, over the 6 wt% catalyst, the conversion of CH_4 was below 20% and only total oxidation of CH_4 occurred. However, the exposed Co surface area of this catalyst after reduction was not negligible (Table 1). This suggests that the initially available metallic sites were oxidized. When the Co loading was increased to 12 wt%, partial oxidation took place. With the increase in Co loading from 12 to 24 wt%, the conversion of CH_4 and the selectivity to CO increased somewhat, but remained almost the same with a further increase from 24 to 48 wt%. The almost equal methane conversions might have occurred either because the reaction was diffusion limited, or because the number of metallic sites (including those generated during reaction) became sufficiently large for thermodynamic equilibrium to be achieved. The results obtained regarding the effect of the amount of catalyst provide useful information in this direction. Indeed, Fig. 4 shows that, for the 1.5 mg of catalyst, the methane conversion was about 86%, with a CO selectivity of about 96%. As the amount of catalyst was increased, the CH_4 conversion and CO selectivity increased, but remained almost unchanged when the amount of catalyst became larger than 5.0 mg. Consequently, the reactions occurred essentially within a thin layer of about 5.0 mg (or even less) at the beginning of the catalyst bed and equilibrium was reached.

5. SUMMARY

The structural characteristics of the Co catalysts are strongly affected by the nature of the support, calcination temperature, and Co loading, and so are their reducibility and catalytic performance. Among the alkaline earth metal oxides (MgO, CaO, SrO, and BaO)-supported Co catalysts (precalcined at 800°C), only Co/MgO has proved to be a highly efficient and stable catalyst. It provided a CH_4 conversion of 91% and a CO selectivity of 98% at the high space velocity of 720,000 ml g^{-1} h^{-1}, without any deactivation for the duration of the experiment (120 h). A solid solution of CoO and MgO was identified in the 800°C calcined MgO-supported catalyst, which is responsible for its superior activity. Due to its low reducibility, the metal crystallites formed during the reduction of the solid solution were small and hence little carbon deposition occurred. Originating from a solid solution, the crystallites were partially embedded into the substrate and thus were resistant to sintering. The reaction behavior of Co/MgO catalysts was strongly affected by the calcination temperature and Co loading. Deactivation was noted for the low calcination temperatures of 500 and 700°C. Besides the solid solution, Co_3O_4 and $MgCo_2O_4$ were identified in the 500°C calcined catalyst and Co_3O_4 in the 700°C calcined one, compounds which can be more easily reduced than the solid solution. The relatively large metal particles, formed during the reduction of the more reducible Co-containing species (Co_3O_4 and $MgCo_2O_4$), stimulated carbon deposition. For calcination temperatures $\geq$800°C, the activity decreased with increasing calcination temperature. Since only the solid solution was present in the catalysts calcined at $\geq$800°C, the higher the calcination temperature the deeper was the penetration of CoO into the MgO lattice. For this reason, fewer metallic sites were present on the surface of the catalysts precalcined at higher temperatures.

REFERENCES

1. Prettre, M., Eichner, C., and Perrin, M., *Trans. Faraday Soc.* **43**, 335 (1946).
2. Hickman, D. A., and Schmidt, L. D., *J. Catal.* **138**, 267 (1992).
3. Bhattacharaya, A. K., Breach, J. A., Chand, S., *et al., Appl. Catal. A: Gen.* **80**, L1 (1992).
4. Hickman, D. A., and Schmidt, L. D., *Science* **259**, 343 (1993).
5. Torniainen, P. M., Chu, X., and Schmidt, L. D., *J. Catal.* **146**, 1 (1994).
6. Nakagawa, K., Ikenaga, N., Suzuki, T., *et al., Appl. Catal. A: Gen.* **169**, 281 (1998).
7. Fathi, M., Hofstad, K. H., Sperle, T., *et al., Catal. Today* **42**, 205 (1998).
8. Ruckenstein, E., and Wang, H. Y., *J. Catal.* **187**, 151 (1999).
9. Dissanayake, D., Rosynek, M. P., Kharas, K. C. C., and Lunsford, L. H., *J. Catal.* **132**, 117 (1991).
10. Vermeiren, W. J. M., Blomsma, E., and Jacobs, P. A., *Catal. Today* **13**, 427 (1992).
11. Choudhary, V. R., Rajput, A. M., and Prabhakar, B., *J. Catal.* **139**, 326 (1993).
12. Tang, S., Lin, J., and Tan, K. L., *Catal. Lett.* **51**, 169 (1998).
13. Tsipouriari, V. A., Zhang, Z., and Verykios, X. E., *J. Catal.* **179**, 283 (1998).
14. Provendier, H., Petit, C., Estournès, C., *et al., Appl. Catal. A: Gen.* **180**, 163 (1999).
15. Ruckenstein, E., and Hu, Y. H., *Appl. Catal. A: Gen.* **183**, 85 (1999).
16. Slagtern, Å., Swaan, H., Olsbye, U., *et al., Catal. Today* **46**, 107 (1998).
17. Santos, A., Menéndez, M., Monzón, A., *et al., J. Catal.* **158**, 83 (1996).
18. Sokolovskii, V. D., Coville, N. J., Parmaliana, A., *et al., Catal. Today*, **42**, 191 (1998).
19. Ashcroft, A. T., Cheetham, A. K., Foord, J. S., *et al., Nature* **344**, 319 (1990).
20. Jones, R. H., Ashcroft, A. T., Waller, D., *et al., Catal. Lett.* **8**, 169 (1991).
21. Slagtern, A., and Olsbye, U., *Appl. Catal. A: Gen.* **110**, 99 (1994).
22. Lago, R., Bini, G., Pena, M. A., and Fierro, J. L. G., *J. Catal.* **167**, 198 (1997).
23. Ruckenstein, E., and Hu, Y. H., *Appl. Catal. A: Gen.* **133**, 149 (1995).
24. Ruckenstein, E., and Hu, Y. H., *Ind. Eng. Chem. Res.* **37**, 1744 (1998).

25. Hagan, A. P., Lofthouse, M. G., Stone, F. S., and Trevethan, M. A., *in* "Preparation of Catalyst II" (B. Delmon, P. Grange, P. A. Jacobs, and G. Poncelet, Eds.), p. 417. Elsevier, Amsterdam, 1979.
26. Gazzoli, D., Occhiuzzi, M., Cimino, A., Cordischi, D., Minelli, G., and Pinzari, F., *J. Chem. Soc. Faraday Trans.* **92**, 4567 (1996).
27. Chung, K. S., and Massoth, F. E., *J. Catal.* **64**, 320 (1980).
28. Arnoldy, P., and Moulijn, J. A., *J. Catal.* **93**, 38 (1985).
29. Náray-Szabó, I., "Inorganic Crystal Chemistry." Akadémiai Kiadó, Budapest, 1969.
30. Rostrup-Nielsen, J. R., *in* "Catalysis Science and Technology" (J. R. Anderson and M. Boudart, Eds.), Vol. 5, pp. 1–118. Springer, Berlin, 1984.
31. Parmaliana, A., Arena, F., Frusteri, F., *et al., J. Catal.* **141**, 34 (1993).
32. Highfield, J. G., Bossi, A., and Stone, F. S., *in* "Preparation of Catalyst III" (G. Poncelet, P. Grange, and P. A. Jacobs, Eds.), p. 181. Elsevier, Amsterdam, 1983.